



Energy, Resources and Environmental Technology

Mathematical model of absorption and hybrid heat pump



Grazia Leonzio

Department of Industrial and Information Engineering and Economics, University of L'Aquila, Via Giovanni Gronchi 18, 67100 L'Aquila, Italy

ARTICLE INFO

Article history:

Received 27 November 2016

Received in revised form 4 June 2017

Accepted 5 June 2017

Available online 4 July 2017

Keywords:

Absorption heat pumps

Hybrid heat pumps

LiBr–H₂O modeling

Energy efficiency

Process simulation

Mathematical model

ABSTRACT

Recovering waste heat from industrial processes is beneficial in order to reduce the primary energy demands and heat pumps can be used to this purpose. Absorption heat pumps are energy-saving and environment-friendly because use working fluids that do not cause ozone depletion and can reduce the global warming emissions. The hybrid heat pump processes combine the conventional vapor-compression and the absorption heat pump cycles. Studies about the simulations and modeling of hybrid heat pumps are few in literature. In this research a mathematical model for single effect absorption and hybrid heat pump is carried out with ChemCad® 6.0.1. LiBr–H₂O is used as working fluid while electrolytic NRTL and electrolytes latent heat are used as thermodynamic model due to the better results. Binary parameters of activity coefficients are regressed from experimental vapor pressure data while default constants are used for the solubility expressions. A design of heat pumps is developed and a new modeling of generator is analyzed. The coefficient of performance of absorption heat pump and hybrid heat pump is equal to 0.7 and 0.83 respectively. For absorption heat pump a sensitivity analysis is carried out to evaluate the effect of temperature and pressure generator, the concentration of Li–Br solution on coefficient of performance, cooling capacity and working fluid temperature. For hybrid heat pump, the different coefficients of performance, the primary energy ratio, the generator heat, and the compressor power are analyzed for different values of compressor proportion. Results show that comparing the two systems the hybrid pump allows to save more primary energy, costs and carbon dioxide emissions with respect to absorption heat pump with the increasing of compressor proportion parameter. Future researches should focus on the construction of this heat pumps integrated in chemical processes as a biogas plant or trigeneration systems.

© 2017 The Chemical Industry and Engineering Society of China, and Chemical Industry Press. All rights reserved.

1. Introduction

Global energy demands are increasing and concerns of global warming brings major challenges considering the future of energy production and consumption. Different chemical processes require energy at high temperatures and produce vast amounts of waste heat, often disposed without further use. The recovering of this waste heat is environmentally because it reduces the use of primary energy and so the use of conventional fossil fuels. The heat pump is the only known process that re-circulates the environmental and waste heat back into a heat production process, offering the energy efficient and environmentally friendly heating and cooling. Several types of heat-pumps exist, and they are classified according to the used external power source (mechanical, thermal, chemical, geothermal, solar, etc.). The use of heat pumps allows the reduction of primary energy, operating costs

and CO₂ emissions and then allows to achieve the target of the European Directive 2009/28/EC until the 2020. The heat pump is recognized by the European Union as a solution to have a 20% reduction in greenhouse gas (GHG) emissions, 20% reduction in primary energy and 20% of additional use of renewable energy until 2020 compared to 1990.

In this contest, absorption heat pumps (AHP) have been used since the late 19th century and a large body of scientific and technical literature has been devoted to the fundamental principles, engineering design and application of them [1–3].

Srikhirin *et al.* [4] review several researches about the possible operating configurations of absorption cycles, working fluids and improvement of the processes. These systems are established as an energy-saving and environment-friendly alternative to conventional vapor compression systems since they use working fluids which do not cause ozone depletion and can reduce the global warming emissions [5–7]. In general, absorption heat pumps are used for solar cooling application, air conditioning, heat and power production.

In addition to absorption heat pumps, the hybrid heat pumps are identified as one of the most promising heat pumps technologies.

E-mail addresses: grazia.leonzio@graduate.univaq.it, grazia.leonzio@virgilio.it.

The hybrid heat pump process combines the conventional vapor-compression heat pump cycle and the absorption heat pump cycle and is especially suited for process with large temperature lifts. In general, there are two possible ways of using a hybrid heat system. Firstly, a moderate capacity compressor can be used to improve an absorption system by putting the compressor between the evaporator and the absorber. This mode, can help to improve the operating parameters of an absorption system and allow the exploitation of very low temperature waste heat. Secondly, the efficiency and the capacity of mechanical vapor compressor unit can be improved by taking advantages of working fluid superheat at the compressor exit with an absorption system set in parallel with the compressor. Hybrid heat pump systems are also distinguished by high performances and are flexible, considering capacity control and external changes. The systems, combined with the use of working fluids that are environmentally, are likely to have an important role in the future of heat pump application.

For many of this kind of heat pumps, LiBr–H₂O is the working fluid pair of choice since it is not toxic, has a high enthalpy of vaporization and does not require a rectification step. Other working fluids are reported by Kim and Infante Ferreira [8], Zhang *et al.* [9], Sun *et al.* [10] and Rodriguez and Belman [11], showing the range of activation temperatures, its type of applications and energetic efficiency.

The thermodynamic properties of working pairs have an important influence to energy efficiency of the system and many other parameters can affect the performance of these systems. For these reasons, many mathematical models have been developed for different purposes, such as the simulation of system, the evaluation of potential of working fluid, the optimization and the design.

In literature, there are several works about the modeling of absorption heat pumps with analytical model [11,12] or with the combination of process simulations and optimization tools [14–18]. In addition, many mathematical models are developed for LiBr–H₂O absorption heat pumps [19,20].

Works about the simulations of hybrid heat pumps through chemical software are few in literature and although the principle of the cycle has been known for over a century, little effort has been done to study the subject until recent decades [21,22].

In this research, the simulations of a hybrid heat pump proposed by Ayala *et al.* [23] and of a single effect absorption heat pump are performed using a chemical process software, as ChemCad® 6.0.1.

In this kind of hybrid pump a compressor is set between the evaporator and the absorber to improve the operating parameters of the absorption system and to allow the exploitation of very low-temperature waste heat.

A modeling of LiBr–H₂O working fluid is carried out, regressing the activity coefficients from vapor pressure data according the best thermodynamic model (electrolytic Non Random Two Liquid): the mathematical model is developed for all system. The regression is developed by the chemical software tool.

In addition, can be underlined that respect to literature works, a new modeling of generator in heat pump is developed too. Generator is simulated by flash *e* not by a heat exchanger to better simulate the separation of refrigerant and absorbent. Comparing the two analyzed systems, the hybrid heat pump allows to save more primary energy, costs and to reduce the carbon dioxide emissions respect to absorption heat pump, with the increasing of compressor proportion parameter. A sensitivity analysis is developed to study the efficiency of two heat pumps. For absorption heat pump the coefficient of performance (COP) and cooling capacity are analyzed varying the temperature and pressure generator and the concentration of Li–Br solution, also the working fluid temperature is studied varying its concentration and the generator pressure. For hybrid heat pump, the different COPs, the primary energy ratio, the generator heat and compressor power are analyzed for different values of compressor proportion (CP). These results can be used to optimize the future construction of the systems and to verify the environmental, economic and energy advantages of hybrid systems.

2. Modeling of Heat Pumps

To study an absorption heat pump through chemical software, it is necessary to model the equipment of the heat pump and the working fluid to calculate the physical chemical properties. To this purpose, a thermodynamic model is set to calculate the activity coefficients that allow to have the physical chemical properties. This concept is developed in this research, using an innovative model of the generator of heat pump. For a better comprehension, it is useful to have a knowledge in this field. In literature, different works are reported about the modeling of absorption heat pumps through software, mathematical equations and about the thermodynamic model to describe the overall system.

2.1. Modeling of working fluid for heat pumps

Many thermodynamic models are developed to calculate the activity coefficients of electrolyte solutions that are present in working fluid of heat pumps in order to predict the equilibrium phase: the development of these models continues to be an important subject for research.

The first of them is the Bromley model and is presented as an empirical expression while the others are based upon a theoretical background.

The Debye–Hückel model is the first model employed to predict the phase behavior of aqueous electrolytes but for very dilute solutions [24].

Guggenheim [25], based on earlier works of Bronstedt *et al.* [26], suggests an empirical extension introducing a specific coefficient for the interactions between cations and anions.

In addition Bromley *et al.* [27] suggest a one-parameter equation that is found empirically by fitting experimental data. Then using the pressure equation for the statistical thermodynamics, Pitzer [28] points out that the interaction coefficient is a function of the ionic strength. Recently, different equations are proposed, based on a local-composition model such as the Uniquac, NRTL and Wilson models.

Cruz and Renon [29] combine the Debye–Hückel expression with the NRTL and Born model contribution, taking into consideration the change of the dielectric constant with salt concentration: four adjustable parameters are necessary to describe a system containing one solvent and one salt.

A similar approach is suggested by Ball *et al.* [30] but with respect to the model of Cruz and Renon, the calculation of the Born contribution provides one adjustable parameter for one binary system.

Chen *et al.* [31] combine the electrostatic function of the Pitzer model with a local composition term, which is an extension of the NRTL equation to electrolyte solutions.

In this contest, Haghtalab and Vera [32] adopt the general ideas of Chen using the original Debye–Hückel expression instead of the Pitzer–Debye–Hückel formula, and they express the local composition through non-random factors. Also, Liu *et al.* [33] introduce a modified Debye–Hückel term, which covers only the long-range interactions between the central ion and all ions outside the first coordination shell. The electrostatic interactions between ions within the first coordination shell are included in the short-range contribution, which is based on a previous derivation of the three-parameters [34,35].

Several excellent reviews of electrolyte solution models are available in literature: empirical and semi-empirical model are reviewed by Zemaitis *et al.* [36], Renon [37], Pitzer [38], Rafal *et al.* [39] and Loehe and Donohue [40]. Theoretical fundamentals are reviewed by Conway [41], Mazo and Mou [42]. These thermodynamic models are implemented in chemical software for the simulation and modeling of heat pumps: infect, with the rapid development of computer science and technology, simulating calculation has become the third main way of modern scientific research.

2.2. Modeling of heat pumps systems

Several system-specific computer models have been developed in order to prove very valuable tools for research, development and design of heat pumps [43–47]. Some of those models are validated against experimental results with good agreement. However, most of them are restricted to a specific system and are empirically derived and in some cases overly simplified.

Marcos *et al.* [48] develop a simulation program to calculate the optimal COP for a water-and air-cooled single and double effect LiBr–H₂O absorption chillers, the percentage of refrigerant vapor generated in the high and low temperature desorbers and the mass flow of the solution for each desorber. Similarly, work is carried out by Gomri [49].

Systematic methods based on mathematical programming techniques as linear (LP), non-linear (NLP), mixed integer linear (MILP) and mixed integer non-linear programming (MINLP) problems are used allowing the optimization of energy conversion systems [50–54]. In addition, mathematical programming environments such as GAMS [55], gPROMS [56], and AMPL [57] are involved.

Mazzei *et al.* [58] develop a non-linear programming mathematical model to determine the operation conditions and the total heat transfer area for a single effect absorption heat pump with LiBr–H₂O, in order to maximize the COP. Other models minimizing operating and investment costs are developed by Kodal *et al.* [59–61], Misra *et al.* [62–64], Sahin and Kodal, [65], Kizilkan *et al.* [66], Palacios Bereche *et al.* [67], Varani *et al.* [68], Sahoo *et al.* [69], Al-Otaibi *et al.* [70].

Mathematical modeling with environmental concerns has received little attention to date.

Simulations of dynamic models of absorption heat pumps are developed by many authors: dynamic simulation plays an important role in the description of the real performance of an energy conversion system, especially during the activation stage or part-load operation. Such a problem is extremely relevant for absorption chillers, where the high mass of internal components and the accumulation of the fluids inside the vessels usually make the transient phase longer than the mechanical compression chillers [71–83].

Simulations are also conducted in steady state conditions too [84].

Alva *et al.* [85] investigate the technical feasibility of a compact air-cooled solar assisted absorption system using computer simulation modeling. Results show that air-cooled absorption machines could have the great advantage of reducing maintenance and cost compared to conventional water cooled. Sencan *et al.* [86] and Arora and Kaushik [20] develop a simulation program to determine the operating conditions that increase both the coefficient of performance and the total exergetic efficiency of a single effect LiBr–H₂O system.

Kaynakli and Kilik [13] show that the COP values increase with the increase of generator and evaporator temperatures but decrease with the increase of condenser and absorber temperatures for a single effect LiBr–H₂O.

Kaynakli and Yamankaradeniz [84] study the performance of LiBr–H₂O system varying some design parameters to determine the entropy generation of individual components and of all system.

Aphornratana and Sriveerakul [85] investigate the performance of single-effect absorption refrigerator using LiBr–H₂O: the experimental COP is found to be approximately the 80% of the theoretical COP due to the low mass transfer performance of the absorber.

Darwish *et al.* [7] simulate an absorption refrigeration chiller using Aspen Plus simulator. The predicted results of various performance parameters are compared with the experimental and some manufacturer data reported in the literature so the agreement is good.

Sun *et al.* [10] analyze the influence of the geometry and the operation parameters on thermal performance for a single effect absorption heat pump.

Karamangil *et al.* [86] carry out a thermodynamic analysis of absorption heat pumps using encountered solution pairs presented in literature and develop an user friendly software package. They find that the performances of the cycle improve with the increasing of generator and evaporator temperatures, but they reduce with the increasing of condenser and absorber temperatures.

Modeling of hybrid absorption heat pumps is few in literature.

Klein *et al.* [87] simulate the annual performances of several hybrid systems with different heat pump sizes, considering two buildings and in a cold climate. Similar research is carried out by Bagarella *et al.* [88] for a residential building: the main economic advantages of a hybrid system come from the lower annual electric and gas energy needs.

3. Materials and Method

3.1. Absorption and hybrid heat pumps

Compared to a compression cooling cycle, the basic idea of an absorption system is to replace the electricity consumption associated with the vapor compression by a thermally driven system, usually known as thermo-chemical compressor. This is accomplished by making use of absorption and desorption process that employs a suitable working pair (refrigerant and absorbent) [4]. The simplest configuration for a single-effect absorption cycle is constituted by a generator, a condenser, an evaporator, an absorber, a heat exchanger, a pump, and two expansion valves, as shown in Fig. 1a. In particular, Fig. 1a shows the single effect LiBr–H₂O absorption cycle in a pressure–temperature diagram. The system provides chilled water for cooling applications and could be activated using available heat from different sources. The basic components are the absorber, condenser, generator and evaporator, solution heat exchanger, refrigerant expansion valve, solution expansion valve and solution pump. It can be seen, when the refrigerant in vapor state comes from the evaporator it is absorbed in a liquid state forming a weak solution. The liquid is pumped to a higher pressure, where the refrigerant is separated from the solution by the

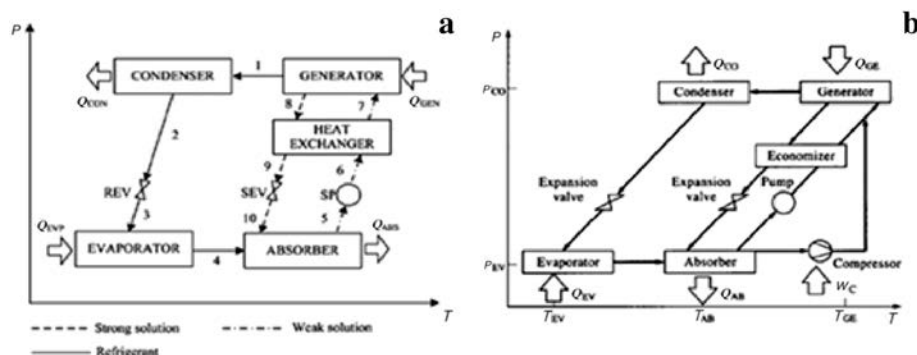


Fig. 1. a) Schematic diagram of a single effect absorption heat pump in PT chart [23]; b) Schematic diagram of hybrid heat pump in PT chart [90].

addition of heat and then the refrigerant is directed to the condenser. Finally, the liquid containing less refrigerant (strong solution) is sent back to the absorber.

Hybrid systems were first suggested over 100 years ago by Ziegler and Hammer [89], Osenbrück [21]. However, during the past 20 years, the development of these systems has been continued towards two main ends. These are increased energy efficiency and the elimination of refrigerants which damage the ozone layer or contribute to the greenhouse effect. The possibility of an absorption/compression (hybrid) system could help reduce the electricity demand in some processes where waste heat is available and to offer the choice of using either high value energy (electricity) or low value energy (waste heat) in order to produce industrial cooling.

Ayala *et al.* [90] propose a hybrid system heat pump shown in Fig. 1b. To the classic cycle absorption a secondary cycle is added, in which the steam produced at the evaporator, instead of proceeding towards the absorber, goes to a compressor: it is compressed to the high pressure and sent to the generator. The addition of this secondary cycle allows to increase the heat pump capacity at the expense of a small electric consumption.

3.2. Thermodynamic model for activity coefficients

The system LiBr–H₂O used for the simulations is electrolytic: Tables 1 and 2 give some information about the electrolyte reactions (dissociation) and the nature of components.

Table 1

Electrolyte reactions for simulated system in the electrolyte settings of ChemCad 6.0.1®

Electrolyte reactions
LiBr ↔ Li ⁺ + Br [−]
H ₂ O ↔ H ⁺ + OH [−]

Table 2

Components present in the simulated system and inserted in “select components database” of ChemCad 6.0.1®

Component	Phase	Ion type
H ₂ O	Vapor/solvent	—
LiBr	Solid	—
H ⁺	Liquid	Cation
OH [−]	Liquid	Anion
Li ⁺	Liquid	Cation
Br [−]	Liquid	Anion

Electrolytes Non-Random Two Liquid (eNRTL) model is used to calculate the activity coefficients involved in the non-ideal vapor–liquid equilibrium and for compiling and predicting other thermodynamic data.

The electrolytes Non-Random Two Liquid (eNRTL) model proposed by Chen *et al.* [31] is designed to represent the properties of all kinds of electrolyte systems over the entire range of electrolyte concentrations.

In addition, modified equations are presented by Aly and Jaretun [91], Haghtalab and Vera [32], Messnaoui *et al.* [77], Chen *et al.* [92], Jaretun and Aly [93], and Chen *et al.* [94,95]. It is in general a model with local composition and that consists of three contributions. The long-range force contribution is a Pitzer–Debye–Hückel model, which considers the electrostatic interactions of ions, especially at low concentrations. The second part of the model is the Born contribution that is applicable to mixed aqueous–non-aqueous electrolyte solvents. The third part is the local composition NRTL contribution, which is

employed for short-range forces effective at higher concentrations of ions. The unsymmetric Pitzer–Debye–Hückel (PDH) model and Born equation are used to represent the contribution of long range ion-ion interactions, and the symmetric NRTL theory is used to represent the local interactions. The excess Gibbs energy, used to calculate the activity coefficients is according the following relation (see Eq. (1)) [32]:

$$G_m^E / RT = G_m^{E,PDH} / RT + G_m^{E,Born} / RT + G_m^{E,LC} / RT \quad (1)$$

The main mathematical expression of the model is (see Eq. (2)):

$$\ln \gamma_i^* = \ln \gamma_i^{*,PDH} + \ln \gamma_i^{*,E,LC} \quad (2)$$

where γ_i^* is the unsymmetrical activity coefficient of ionic species i and the first and second terms on the right side of the above equation are the activity coefficients introduced by the Pitzer–Debye–Hückel and NRTL local composition models, respectively [96]. For an apparent binary aqueous electrolyte system, the binary parameters are expressed as $\alpha_{ca,w}$, $\tau_{ca,w}$, $\tau_{w,ca}$, where $\alpha_{ca,w}$, the non-randomness parameter, has a value ranging from 0.1 to 0.5. The other two parameters are energy parameters and are written in terms of temperature as following relations (see Eqs. (3) and (4)):

$$\tau_{ca,w} = A_{ca,w} + B_{ca,w} / T + C_{ca,w} \cdot \left[(T^\circ - T) / T + \ln(T / T^\circ) \right] \quad (3)$$

$$\tau_{w,ca} = A_{w,ca} + B_{w,ca} / T + C_{w,ca} \cdot \left[(T^\circ - T) / T + \ln(T / T^\circ) \right] \quad (4)$$

where T° is the reference temperature of 298.15 K. The subscript “ca” and “w” denote the electrolyte (cation–anion) and solvent (water, in general), respectively. Thus, for an apparent binary electrolyte system with a fixed non-randomness parameters, for each interaction energy parameter τ , three adjustable parameters A , B and C should be calculated over the whole range of temperatures. Chen and Evans [31] gives the eNRTL expression for the activity coefficient of cations and anions in an apparent binary electrolyte system.

The advantages of the eNRTL model are the general temperature dependence of ion interaction parameters so it is applicable to a wide range of temperatures.

An experimental procedure is carried out to find the binary interaction parameters for the eNRTL model. Experimental vapor pressure data are used to regress the binary parameters using the tool of ChemCad. In fact, this software allows the regression of the binary interaction parameters for different thermodynamic models by the experimental data of the physical properties of the binary mixtures (solubility, vapor pressure or density data). To verify the realized thermodynamic model, the vapor pressure data obtained by simulation are compared with the experimental one. The calculated binary interaction parameters are set inside the software and a flash is used to generate the vapor pressure data according the model.

In this work, the regression of binary parameters for LiBr–H₂O system is carried out using the experimental vapor pressure data (MPa) obtained from the semi-empirical correlation proposed by Sun *et al.* [97] where the vapor pressure is related to the temperature and concentration solution (see Eq. (5)):

$$p^{\text{vap}} = \exp \left(-396806 / T - 395735 + \sum_{i=0}^9 a_i T_d^i \right) \quad (5)$$

where a_i are experimental parameters, T is the solution temperature (°F, $T/^\circ\text{F} = (T/^\circ\text{C}) \times 1.8 + 32$), T_d is the dew point temperature of the solution (°F) calculated from the following equation [97] (see Eq. (6)):

$$T_d(T, x_{\text{LiBr}}) = \sum_{i=0}^5 \sum_{j=0}^2 a_{ij} x_{\text{LiBr}}^i T^j \quad (6)$$

where a_{ij} are experimental data, x_{LiBr} is the weigh concentration of LiBr in water, T is the solution temperature (°F, $T/^\circ\text{F} = (T/^\circ\text{C}) \times 1.8 + 32$). For

calculating the vapor pressure, x_{LiBr} varies in the range of 42.5wt% and 62.5wt%, while the temperature solution between 283 K and 373 K for every concentration. As explained below, the concentration solution is chosen in order to avoid crystallization phenomena during the operation of the heat pump and to model all conditions inside the two critical conditions, that can be during the operation of heat pump.

Table 3 shows the regressed binary parameters calculated by the software, for the components in the system, each of which forms a central cell surround by another species. Based on the eNRTL assumptions, only counter ions and molecular species interact with corresponding ions sited in the center of the cells and local electro-neutrality applies to molecular central cells. In the table, the subscripts m, c, and a stand for molecule (m), cation (c), and anion (a), respectively; $\tau_{m,ca}$ is the molecule–electrolyte interaction parameter while $\tau_{ca,m}$ is the electrolyte–molecule interaction parameter. For each interaction, energy parameters τ , A , B and C are the coefficients according to Eqs. (3) and (4) while $\alpha_{ji,ki}$ represents the non-randomness factors.

Table 3

Regressed binary parameters for electrolyte system according to electrolyte non-random two liquid model

m	c	a	$\tau_{m,ca,A}$	$\tau_{m,ca,B}$	$\tau_{m,ca,C}$	$\tau_{ca,m,A}$	$\tau_{ca,m,B}$	$\tau_{ca,m,C}$	Alpha
H ₂ O	Li ⁺	Br [−]	12	55	−836	−5	−891	−2	0.052
H ₂ O	H ⁺	Br [−]	22	−2987.4	0	−5	−236	0	0.206
H ₂ O	LiBr	0	−9	398	0	0	0	0	0.013
Br [−]	Li ⁺	Li ⁺	−408	498	24	0	0	0	0.2
Li ⁺	Br [−]	Br [−]	971	−750	−107	0	0	0	0.2

The obtained values are set inside the software to generate the vapor pressure data for the mixture using a flash. Then, the results are evaluated utilizing Microsoft Excel Software (2011) and the regression analysis of the data, shown in Fig. 2, provides the following equations (see Eq. (7)).

$$Y = 0.97 \cdot X - 0.09 \quad (R^2 = 0.99) \quad (7)$$

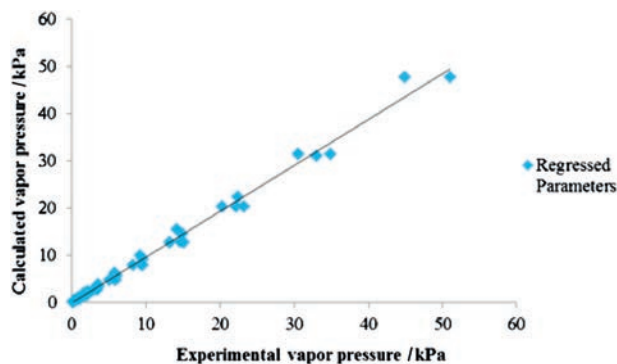


Fig. 2. Linear regression of vapor pressure data for LiBr–H₂O system with eNRTL model.

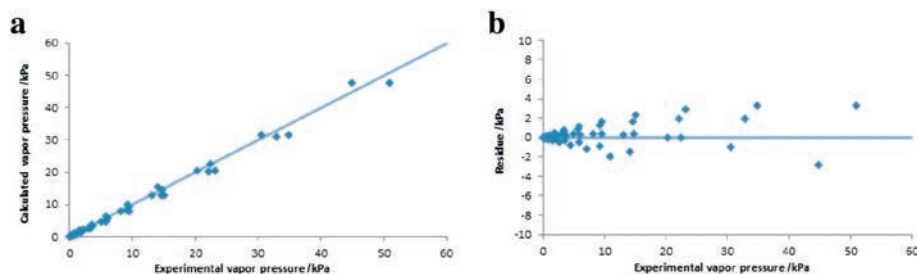


Fig. 3. a) Scatter diagram of calculated vapor pressure data versus the experimental vapor pressure data of LiBr–H₂O system; b) Residue diagram versus experimental vapor pressure data of LiBr–H₂O system.

This empirical equation is suitable to predict the vapor pressure in the range of the studied experimental conditions for process optimization purposes. In this calculation, the concentration of solution varies between 42.5wt% and 62.5wt% and for each composition the temperature varies between 283 K and 373 K. The maximum value of vapor pressure obtained is equal 51×10^5 Pa.

The comparisons among the experimental vapor pressure data and the estimated ones by regression model are shown in the scatter and residue diagram (Fig. 3a and b respectively). The results suggest that there is a good agreement between the predicted and the measured vapor pressure data, so the regressed binary parameters for eNRTL thermodynamic model are corrected.

These activity coefficients can be set in other process simulators to model these kinds of absorption heat pumps.

Considering Pitzer electrolyte model and its regressed binary parameters $\beta^{(0)}, \beta^{(1)}, \beta^{(2)}$ [98], it is found that this thermodynamic model is not able to assess the increase of the boiling temperature with the increase of LiBr concentration in water. Figs. 4 and 5 and Table 4 show the excellent performance of eNRTL over the Pitzer model, considering only binary parameters that exist in the default ChemCad 6.0.1® databank.

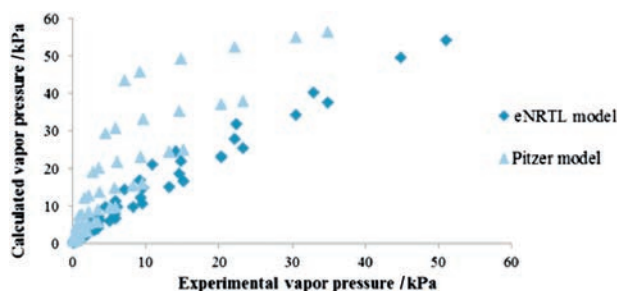


Fig. 4. Comparison of eNRTL and Pitzer model considering vapor pressure data of LiBr–H₂O system.

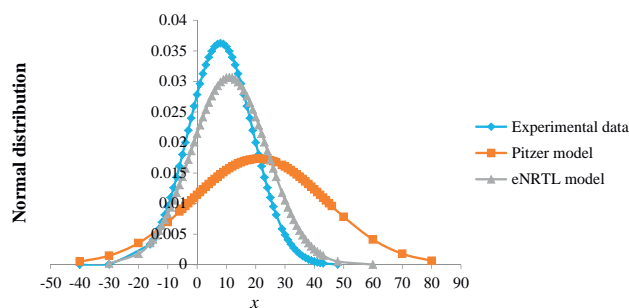


Fig. 5. Normal distribution for vapor pressure data of LiBr–H₂O system.

Table 4Statistical analysis for vapor pressure data of LiBr–H₂O according different thermodynamic models

	Experimental vapor pressure	Calculated vapor pressure (Pitzer)	Calculated vapor pressure (eNRTL)
Maximum $\times 10^{-5}/\text{Pa}$	51	82	54
Minimum $\times 10^{-5}/\text{Pa}$	0.06	0.74	0.06
Average	8	21	11
Variance	129	548	166
Standard deviation	11	23	13

3.3. Thermodynamic model for the enthalpy

Electrolytes latent heat is used as enthalpy model for the energy balances involved in the simulations. According to latent heat model, the enthalpies are calculated by the following equation (see Eq. (8)) [98]:

$$H_l = H_{f(l)}^{298.15} + \int_{298.15}^T c_{p,l} dT = H_{l,bubble} + H_{v,at bubble} + \int_{T_{bubble}}^T c_{p,v} dT \quad (8)$$

where: H_l is the liquid enthalpy; $H_{f(l)}^{298.15}$ is the heat of formation of liquid at 298.15 K; $c_{p,l}$ is the liquid heat capacity; H_v is the vapor enthalpy; $H_{l,bubble}$ is the liquid enthalpy at bubble point and system pressure; $H_{v,at bubble}$ is the heat of vaporization at bubble point; $c_{p,v}$ is the heat capacity of vapor. Regarding the electrolyte latent heat used for our simulation, heats of reaction or dissociation are included in the heat balance described above [85].

3.4. Thermodynamic model for the solubility

For the solubility calculation, the default equilibrium constant coefficients for LiBr and H₂O are used and reported in Table 5 according the following equation (see Eq. (9)) [98].

$$K_{eq} = A + \frac{B}{T} + C \cdot \ln(T) + D \cdot T + E \cdot T^2 \quad (9)$$

where T is the absolute temperature in Kelvin.

Table 5

Parameter values of the dissociation equilibrium constants for the compounds insert in ChemCad 6.0.1® (edit electrolyte input-equilibrium)

	A	B	C	D	E
LiBr	0	0	0	0	0
H ₂ O	1.41×10^6	-1.34×10^8	-2.25×10^5	0	0

Accurate data on LiBr solubility in water are required for design and performance prediction of the process, to avoid crystallization phenomena. Available data in literature about the solubility of LiBr in water are very disparate, as shown Fig. 6 [99], where solubility curves are reported in function of the temperature crystallization and the concentration of LiBr.

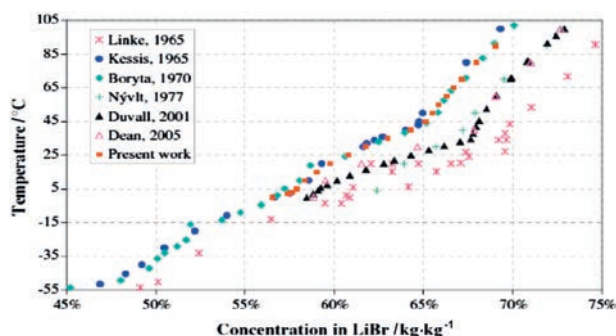


Fig. 6. Li–Br solubility in water as a function of the temperature according to various studies [99].

It is already known, from different studies, that for absorption heat pumps the optimal operating conditions are obtained for concentrations of LiBr at around 50wt% [100,101]. For this research the concentration of LiBr is set to 56wt% with the minimum temperature of the cycle of 303 K (in the absorber), so there are not problems for crystallization of the salts.

4. Results

4.1. Simulation of absorption heat pump

The single effect absorber heat pump is analyzed by simulation program (ChemCad 6.0.1®) and Fig. 7 shows the process scheme in the calculation environment.

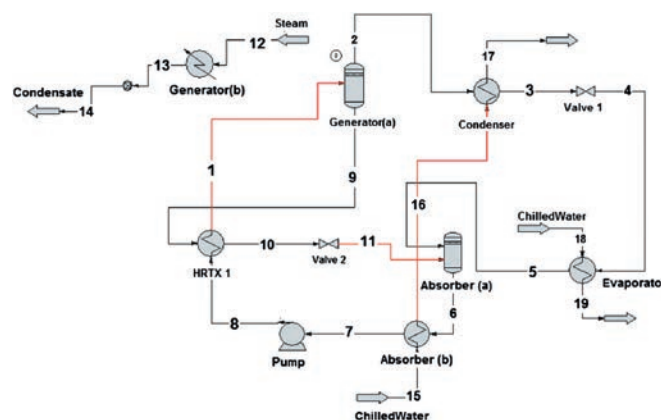


Fig. 7. Process simulation of absorption heat pump: plant operation scheme in ChemCad 6.0.1® environmental.

Generator is simulated by flash and not by a heat exchanger to better simulate the separation of refrigerant and absorbent. It is divided in flash tank (generator a) and heat exchanger (generator b), to calculate the necessary steam for vaporization and then to drive the absorption heat pump. Absorber is divided in two parts: absorber a and absorber b. The two stream from evaporator and generator enter in the flash (absorber a) where the heat of reaction is developed for the dilution of LiBr solution. This heat is removed in the heat exchanger (absorber b). Then the two sets of equipment allow to model the two streams that enter in the absorber and develop a heat of reaction due to the dilution of the Li–Br solution and this heat is removed by the heat exchanger.

Refrigerant is used in the absorber and the evaporator has chilled water. In the first case, chilled water enters in the absorber and then in the condenser to increase the thermal level of cooling water. This arrangement is due by the absorber temperature that is lower than the condenser temperature, allowing a better efficiency for the two heat exchangers. Table 6 shows the material and energy balances obtained by the simulation while Table 7 shows some operating data set by literature and sensitivity analysis in order to obtain a high COP. This values are set then to simulate the absorption heat pump and to generate the material and energy balances. The simulations are carried out in steady-state conditions, with the default relative convergence error tolerance of 0.01%.

For a better study of the absorption heat pump, a sensitivity analysis is carried out, modifying the generator temperature and pressure. Generator temperature is a fundamental parameter for absorption heat pump [100], because it influences the vapor fraction and then the amount of the produced steam. At a fixed value of the generator pressure, varying the generator temperature, the vapor fraction is changed and then other parameters of the heat pump chosen as responses in

Table 6
Material and energy balances of the absorption heat pump obtained by the simulation with ChemCad 6.0.1® (see Fig. 7)

Number stream	1	2	3	4	5	6	7	8	9	10	11	12	13	14	15	16	17	18	19
Temperature /K	337	358	308	276	278	317	306	306	358	316	316	415	369	369	299	303	306	285	281
Pressure $\times 10^{-5}$ /Pa	6.15	6.15	6.15	0.76	0.76	0.76	0.76	0.76	6.15	6.15	6.15	200	200	200	300	300	300	303	303
Vapor fraction	0	1	0	0.05	1	0.11	0	0	0	0	0	1	0	0	0	0	0	0	0
Enthalpy ^(a) (kcal·h ⁻¹)	-1.4×10^7	-2.3×10^6	-2.7×10^6	-2.7×10^6	-2.3×10^6	-1.4×10^7	-1.4×10^7	-1.4×10^7	-1.2×10^7	-1.2×10^7	-1.2×10^7	-1.2×10^7	-3.2×10^6	-3.2×10^6	-4.9×10^8	-4.9×10^8	-4.9×10^8	-3.8×10^8	-3.8×10^8
Total flow /kg·h ⁻¹	6345	722	722	722	722	6345	6345	6345	5623	5623	5623	852	852	852	129508	129508	129508	49330	101230
H ⁺ /kg·h ⁻¹	0	0	0	0	0	0	0	0	0	0	0	0	0	0	0	0	0	0	0
OH ⁻ /kg·h ⁻¹	0	0	0	0	0	0	0	0	0	0	0	0	0	0	0	0	0	0	0
H ₂ O/kg·h ⁻¹	2785	722	722	722	722	2786	2785	2785	2063	2063	2063	852	852	852	129508	129508	129508	49330	101230
Br ⁻ /kg·h ⁻¹	3275	0	0	0	0	3275	3275	3275	3275	3275	3275	0	0	0	0	0	0	0	0
Li ⁺ /kg·h ⁻¹	284	0	0	0	0	284	284	284	284	284	284	0	0	0	0	0	0	0	0
LiBr/kg·h ⁻¹	0	0	0	0	0	0	0	0	0	0	0	0	0	0	0	0	0	0	0

^(a) 1 kcal = 4.1868 J.

Table 7
Operating conditions of absorption heat pump set in ChemCad 6.0.1®

Parameter	Value	References
Cooling capacity/kW	216	
Concentration solution LiBr/wt%	56	[100]
Generator pressure $\times 10^{-5}$ /Pa	6.15	
Evaporator pressure $\times 10^{-5}$ /Pa	0.76	
ΔT overheating evaporator/K	2	
ΔT sub cooling condenser/K	2	
Generator temperature/K	358	
Absorber temperature/K	306	
Efficiency regenerator	0.8	[8,23]
Coefficient of performance	0.7	

the following graphs. Fig. 8a shows that for a given value of the generator pressure, the COP increases almost vertically with increasing the generator temperature, or rather with increasing vapor fraction, until reaching an asymptotic value. After this value, the generator temperature is not significant for the COP of absorption heat pump. It should be noted that the same behavior is observed by Herold *et al.* [102], Bakhtiari *et al.* [103] and Wu *et al.* [104]. In addition, the COP is higher for lower generator pressure: absorption heat pumps work better with decreasing pressure in the generator. However, with lower

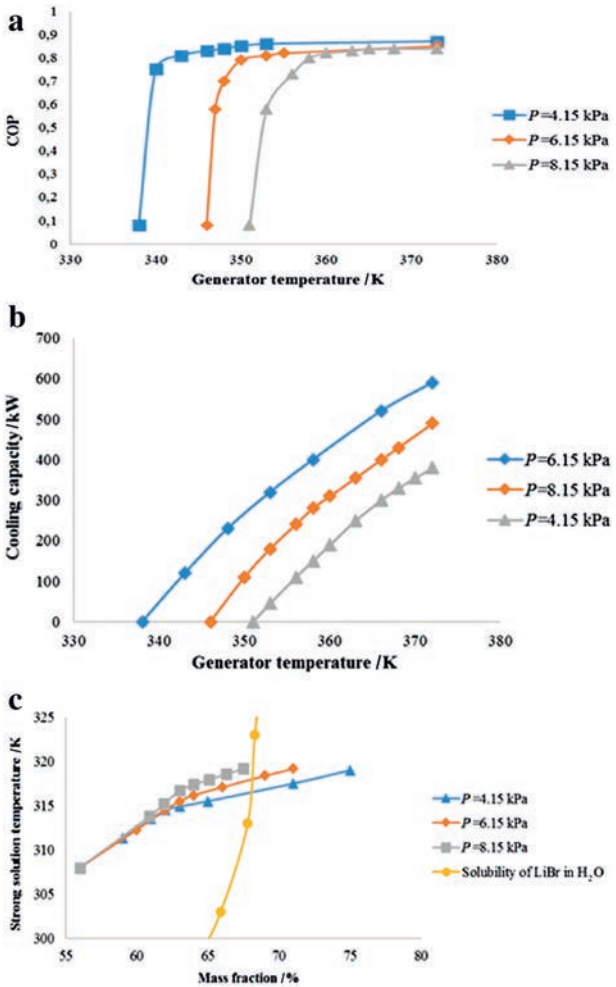


Fig. 8. a) COP versus generator temperature for different values of pressure generator; b) Cooling capacity versus generator temperature for different values of pressure generator; c) study of the conditions in the absorber inlet as function of salt concentration and pressure generator.

pressure the condensation is more difficult and expensive: it is necessary to find an optimal value for this condition.

Fig. 8b shows the cooling capacity versus generator temperature for different generator pressure. Cooling capacity is a linear function of generator temperature for fixed generator pressure: with the higher generator temperature, the amount of steam that is produced is greater and therefore cooling capacity is higher as shown by Bakhtiari *et al.* [103]. Generator pressure has a high influence on cooling capacity: it is possible to have higher cooling capacity with lower generator pressure, for a given generator temperature. This is caused that for a given temperature with a decreasing pressure is greater the amount of produced steam and, therefore, the higher the refrigeration capacity. Fig. 8c is important: shows the concentration of solution versus the strong solution temperature with solubility curve. It is possible to have all operative conditions to the right of solubility curve, avoiding possible precipitation phenomena. The plot does not show the correlation with the generator temperature, but this parameter is related to concentration solution: higher generator temperatures produce higher concentration solution at the inlet of the absorber. The concentration temperature curves can be divided in two parts. In the first part where the curves overlap, the strong solution is not concentrated excessively: the downstream of the valve has evaporation and the conditions being fixed by the thermodynamic equilibrium are the same for all conditions. In the second part, with increasing concentration in the generator (increased temperature), the evaporation at the downstream of the valve disappears and therefore the conditions are not determined by equilibrium.

This graph, in Fig. 8c, shows that low pressures increase the vaporization concentrating solutions and producing problems of precipitations at the downstream of the valve. For this reason, the generator does not work with low pressures too. In addition, the temperature-concentration plots increase rapidly at the first and then increase slower creating an angular point. This is because in the first part where the curves overlap the strong solution is not concentrated excessively: at the downstream of the valve the evaporation is present and the conditions being fixed thermodynamic equilibrium are the same. With higher concentration in the generator (with the higher temperature), the evaporation at the downstream is not present and therefore the conditions are determined by different equilibrium parameters. The plot shows the reason for which the generator pressure is not low: lower pressures increase the vaporization concentrating the solution with precipitating problems at the downstream of the valve. The points at the right side of the solubility curve are not significant because the operation of the heat pump is not possible; they are calculated in theory during the simulation.

Comparing Figs. 8c and 6 it is evident that the implemented model is correct and validated.

Following graphs show the performance of the heat pump for different value of the concentration of LiBr in water. The characteristics of heat pump are studied varying the generator temperature and the concentration of solution. The aim of this study is not to find the value of the concentration that optimize the performance of heat pump but to evaluate the influence of the concentration solution on the characteristic of heat pump. The concentration of LiBr varies between this values, such as 50wt%-60wt%, in order to avoid crystallization phenomena of the salt. Infact, for an absorption heat pump with a single effect, according the diagram of Dühring and the operating temperature and pressure of the cycle, the concentration of solution must be within a specific range. In particular, as shown in Fig. 9, for a temperature of the cycle between 20 °C and 60 °C the concentration of the salt is between 50wt% and 70wt%. In a Dühring plot, the temperature of the solution is plotted as abscissa on a linear scale, the saturation temperature of pure water is plotted as ordinate on the right-hand side (linear scale) and the pressure on a logarithmic scale is plotted as ordinate on the left-hand side. The plot shows the pressure-temperature values for various constant concentration lines (isosters), which are linear on Dühring plot [105].

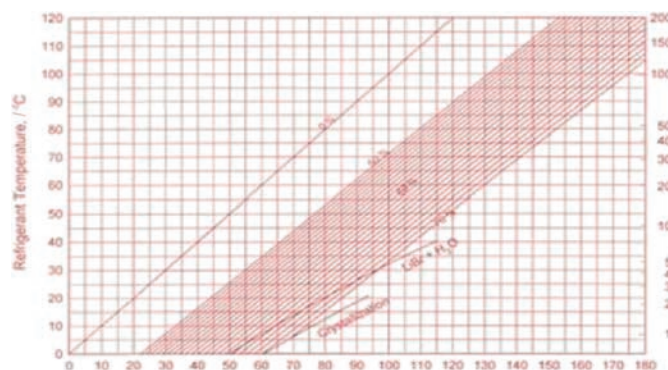


Fig. 9. Dühring diagram of the LiBr-H₂O system.

Fig. 10a shows that COP value increases with the generator temperature and with the decrease of LiBr concentration in solution. At lower concentration, the evaporation requires less heat and so the heat pump has better performance.

The cooling capacity increases with higher generator temperature and lower LiBr concentration, as shown in Fig. 10b. The lower

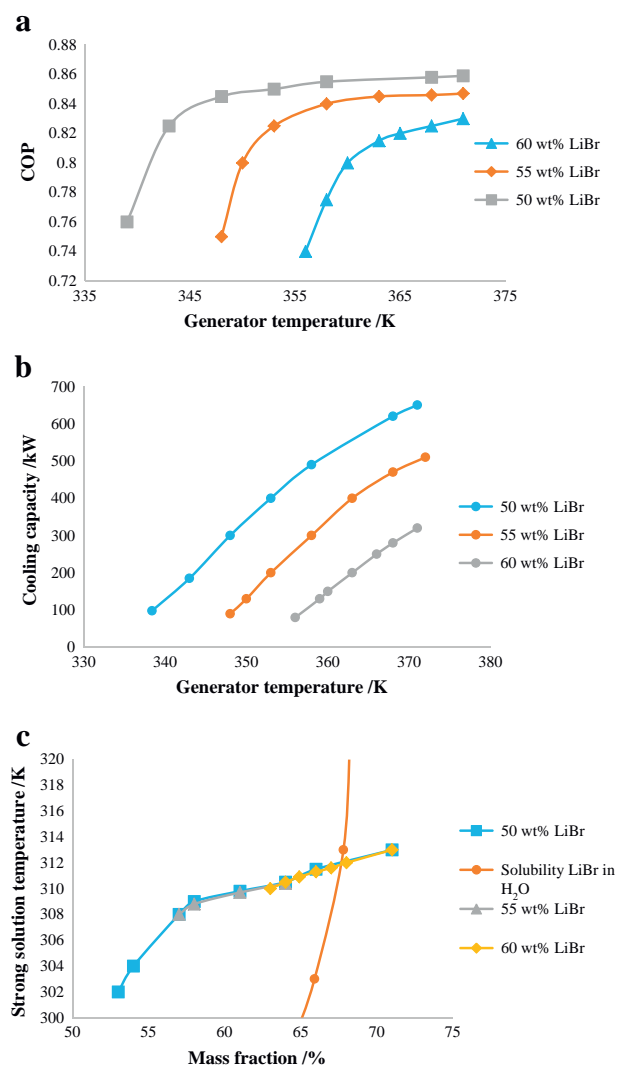


Fig. 10. a) COP versus generator temperature for different values of salt concentration; b) Cooling capacity versus generator temperature for different values of salt concentration; c) Study of the conditions in the absorber inlet as function of salt concentration.

concentration allows a higher vaporization for a fixed temperature, increasing the useful effect provided to the evaporator.

Fig. 10c presents the study of concentration of strong solution entering to the absorber as a function of input temperature to the absorber for different value of LiBr concentration with solubility curve. In this case the curves overlap, because the operating conditions are the same for each condition. Also, in this case, there is the point that divides the angular curve, or the point that distinguishes the conditions in which the valve has evaporation at the downstream (the left of the sharp corner) and the conditions in which the concentration is high to prevent evaporation (to the right of the sharp corner).

4.2. Simulation of hybrid heat pump

Fig. 11 shows the process scheme developed for hybrid heat pumps in the calculation environment of ChemCad 6.0.1®.

For generator and absorber simulations are valid the considerations of absorption heat pump. A compressor is now integrated in the cycle, increasing the efficiency of the system. The compressor is set after the evaporator so part of the produced vapor in the evaporator follows an alternative compression cycle.

In this way, the system exploits the superheat of the working fluid at the compressor exit to add heat to the refrigerant strong solution before it enters to the generator. Higher values of COP are then obtained.

Another hybrid scheme is proposed by Boer *et al.* [22]: a compressor is introduced between the evaporator and the absorber in a double effect absorption cycle for air conditioning using organic working pairs. This compression is expected to increase the temperature lift and the COP, and to decrease the solution circulation ratio and the temperature required in the generator. The temperature in the generator is not increased but only the temperature lifts, so the absorber and condenser can be air cooled.

Table 8 shows the material and energy balances obtained by the simulation while Table 9 some operating data of heat pump, that are obtained by sensitivity analysis or literature data. Simulations are carried out in steady state conditions. Results are comparable with the work of Zhang *et al.* [106].

Hybrid heat pump has two energetic inputs, so there are two different COPs: thermal (COP_{th}) for the operation as absorption heat pump and mechanic (COP_m) for the operation as compression heat pump, as reported in following equations (see Eq. (10)):

$$COP_{th} = \frac{Q_{eva}}{Q_{gen}} \quad COP_m = \frac{Q_{eva}}{W_{com}} \quad (10)$$

where Q_{eva} is the heat released in evaporator, Q_{gen} is the heat supplied to generator and W_{com} is the electric energy of the compressor. The total

coefficient of performance, COP_{tot} , is obtained by following equation [101] (see Eq. (11)):

$$COP_{tot} = \left(\frac{1}{COP_{th}} + \frac{1}{COP_m} \right)^{-1} \quad (11)$$

In general, the COP_{th} is much smaller than the COP_m so it has a higher influence on the COP_{tot} . This parameter is not widely used and it is not based on any thermodynamic, economic or technical law but allow to characterize the performance of an hybrid heat pump with different kinds of energetic inputs [101]. In fact, in literature different expressions for COP of hybrid heat pump are reported in Boer *et al.* [107] and in Sawada *et al.* [108].

Compressor proportion (CP) is another important parameter, defined as the fraction of vapor which is processed by the compressor from the entire amount of steam produced to the generator. This parameter estimates the influence of compression cycle to hybrid cycle; it assumes values between 0 and 1 respectively for operation as absorption and compression heat pump. It is interesting to study the behavior of heat pump varying the amount of steam that flows the compression cycle, which is the amount of steam that is processed by compressor with respect to the total steam produced by the generator.

Fig. 12 shows the different COPs of hybrid pump *versus* compressor proportion.

The thermal COP is strongly influenced by CP and increases with this parameter, with a higher vapor fraction in the compression cycle. A lower heat is required by the generator because this is in part provided by the reduction of temperature steam at the compressor outlet. The mechanic COP decreases with the CP because the compressor consumes a higher power with a greater quantity of sent steam, so the energy efficiency decreases at fixed refrigerant capacity. The total COP is influenced by others: for low values of the CP, the thermal COP influences the energy efficiency of the system, while for high values of the CP the COP_{tot} practically is given by COP_m . When no heat is supplied to generator, the COP_{tot} has a maximum in a limit condition: the heat for the evaporation to the generator is entirely provided by the reduction of steam temperature coming from the compressor. Increasing the CP over this value is necessary to extract heat from the generator, so it has lower values of COP. The limit value of the compressor proportion is equal to 0.9. Fig. 12 shows that the optimal operating condition of hybrid heat pump can be achieved with maximum value of the COP_{tot} . With a CP value of 0.5 the system has the maximum COP equal to 10. In general, for hybrid heat pumps with the increase of generator and evaporator temperature the maximal COP increases, while the optimal compressor ratio decreases [106].

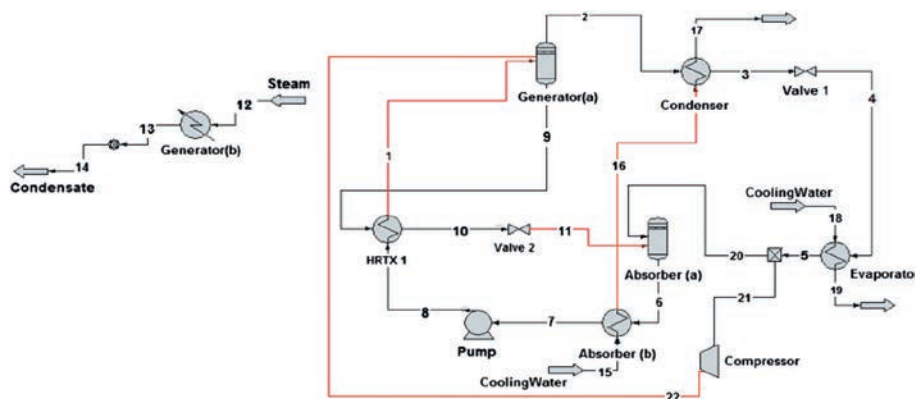


Fig. 11. Process simulation of hybrid heat pump: plant operation scheme in ChemCad 6.0.1® environmental.

Table 8

Material and energy balance of hybrid heat pump obtained by the simulation with ChemCad 6.0.1®

Number stream	1	2	3	4	5	6	7	8	9	10	11
Temperature/K	337	358	308	276	278	317	306	306	358	316	316
Pressure $\times 10^{-5}$ /Pa	6.15	6.15	6.15	0.76	0.76	0.76	0.76	6.15	6.15	6.15	0.8
Vapor fraction	0	1	0	0.1	1	0.1	0	0	0	0	0
Enthalpy ^① /kcal·h ⁻¹	-7.3×10^6	-2.3×10^6	-2.7×10^6	-2.7×10^6	-2.3×10^6	-7.1×10^6	-7.3×10^6	-7.3×10^6	-5.9×10^6	-5.9×10^6	-5.9×10^6
Total flow /kg·h ⁻¹	3172	722	722	722	722	3172	3172	3172	2811	2811	2811
H ⁺ /kg·h ⁻¹	0	0	0	0	0	0	0	0	0	0	0
OH ⁻ /kg·h ⁻¹	0	0	0	0	0	0	0	0	0	0	0
H ₂ O/kg·h ⁻¹	1393	722	722	722	722	1343	1393	1393	1032	1032	1032
Br ⁻ /kg·h ⁻¹	1637	0	0	0	0	1637	1637	1637	1637	1637	1637
Li ⁺ /kg·h ⁻¹	142	0	0	0	0	142	142	142	142	142	142
LiBr/kg·h ⁻¹	0	0	0	0	0	0	0	0	0	0	0

Number stream	12	13	14	15	16	17	18	19	20	21	22
Temperature/K	415	368	368	299	301	306	285	281	278	278	507
Pressure $\times 10^{-5}$ /Pa	200	200	200	300	300	300	303	303	0.76	0.8	6.15
Vapor fraction	1	0	0	0	0	0	0	0	1	1	1
Enthalpy ^① /kcal·h ⁻¹	-1.2×10^6	-1.4×10^6	-1.4×10^6	-3.8×10^8	-3.8×10^8	-3.8×10^8	-3.8×10^8	-3.8×10^8	-1.2×10^6	-1.2×10^6	-1.1×10^6
Total flow /kg·h ⁻¹	382	382	382	100704	100704	100704	101230	101230	361	361	361
H ⁺ /kg·h ⁻¹	0	0	0	0	0	0	0	0	0	0	0
OH ⁻ /kg·h ⁻¹	0	0	0	0	0	0	0	0	0	0	0
H ₂ O/kg·h ⁻¹	382	382	382	100704	100704	100704	101230	101230	361	361	361
Br ⁻ /kg·h ⁻¹	0	0	0	0	0	0	0	0	0	0	0
Li ⁺ /kg·h ⁻¹	0	0	0	0	0	0	0	0	0	0	0
LiBr/kg·h ⁻¹	0	0	0	0	0	0	0	0	0	0	0

① 1 kcal = 4.1868 J.

Table 9

Operating conditions of hybrid heat pump set in ChemCad 6.0.1®

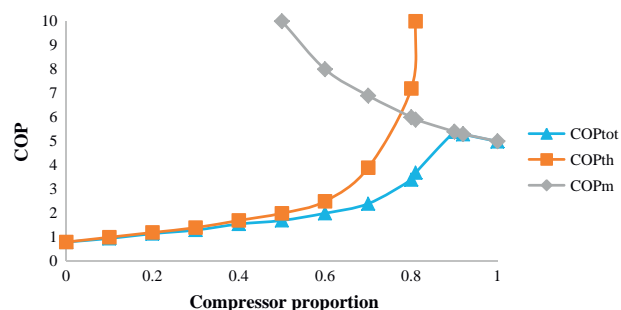
Parameter	Value	References
Cooling capacity/kW	261	
Generator pressure $\times 10^{-5}$ /Pa	6.15	
Evaporator pressure $\times 10^{-5}$ /Pa	0.76	
Concentration solution LiBr/wt%	56	[100]
ΔT overheating evaporator/K	2	
ΔT subcooling condenser/K	2	
Generator temperature/K	358	
Absorber temperature/K	306	
Regenerator efficiency	0.8	[8,23]
Pump efficiency	0.7	
Coefficient of performance	0.83	

For the same pressure ratio, higher generator temperature not only enhances the refrigerant vaporization, but also raises the solution concentration difference, thus favors heat generation. Driven by the increase of both pressure ratio and generator temperature, the solution concentration difference increases more rapidly, and the optimal COP is reached at lower pressure ratio. When the evaporator temperature increases, the evaporation pressure increases as well, leading to the reduction of the total compression requirement, thus the fraction of mechanical compression reaches a higher level although the absolute compressor ratio is still low.

Other important parameters for hybrid heat pump are the primary energy ratio, PER (the relation between useful energy output divided by necessary energy input) and the heat and electrical energy supplied to the generator and compressor respectively. There are energetic diagrams to underline the advantages that hybrid pump has with respect to absorption heat pump.

The PER gives a direct value of the overall efficiency for a complete system, taking into account for the losses related to the generation of electricity. PER is the highest for direct power generation from renewable sources such as hydro, wind or solar.

As shown in Fig. 13, the PER is linear with the CP and decreases until minimum value (the limit condition described above) where the hybrid

**Fig. 12.** COP thermal, COP mechanic, COP total of hybrid heat pump versus compressor proportion.

heat pump works with the maximum efficiency. It is evident that with higher compressor proportion the primary energy ratio decreases, because more losses are present.

The heat supplied to generator has a linear decreasing with compressor proportion, while compressor power has a linear increasing with CP, as Fig. 14 shows.

Fig. 15 compares the two analyzed heat pumps respect to primary energy, costs and carbon dioxide emissions. Fig. 15a shows the primary energy saving that hybrid heat pump allows to have over absorption heat pump, versus compressor proportion. The primary energy is calculated as tep (ton of equivalent of petroleum) per year regarding the consumed methane and electrical energy of the systems. From a comparison of two systems is preferable to use PER and not COP, because hybrid pump has two different COPs (thermal and mechanical) with two different energetic inputs. The hybrid pump allows to save more primary energy whit increasing of compressor proportion. The hybrid cycle has therefore improved the ability to use and upgrade low-temperature heat as compared with either cycle. The same considerations are valid for the saving of operative costs and carbon dioxide emissions, shown in Fig. 15 b and c. The operative costs are related to methane (for the production of the steam for the generator) and

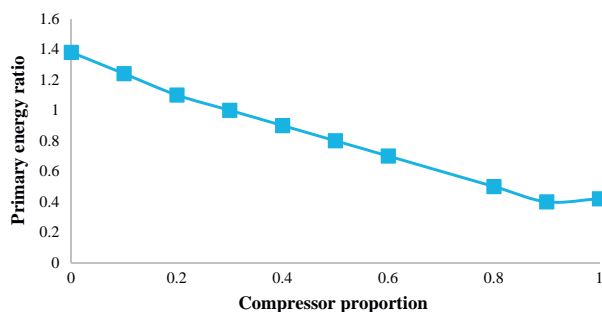


Fig. 13. Primary energy ratio of hybrid heat pump versus compressor proportion.

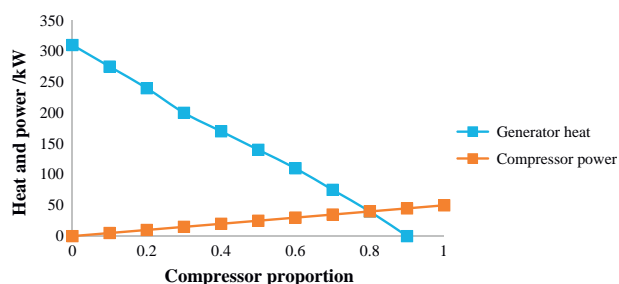


Fig. 14. Generator heat and compressor power of hybrid heat pump versus compression proportion.

electrical energy (for compressor and pumps) considering a price equal to $0.54 \text{ EUR} \cdot \text{S}^{-1} \cdot \text{m}^{-3}$ and $0.15 \text{ EUR} \cdot \text{kW}^{-1} \cdot \text{h}^{-1}$ respectively with an operation time of the system equal to 7200 h per year. According to this, the carbon dioxide emissions are related to the consumed methane and electrical energy. The presence of a limit value for the compressor proportion influences the trend of these plots. It is evident, that the hybrid heat pump allows having the higher advantage respect to a conventional absorption heat pump. The hybrid heat pump provides energetic, environmental and economic advantages with respect to a conventional absorption heat pump. In particular, in correspondence to the compressor proportion limit value, it allows to save the 57%, 70%, and 67% of costs, primary energy and carbon dioxide emissions respectively. The higher primary energy saving allows to have higher economic incentives as the white certificates.

5. Conclusions

Absorption heat pumps have been used since the late 19th century and a large body of scientific and technical literature has been devoted to the fundamental principles, engineering design and application of those devices. Also, due to volatile energy prices and environmental concerns, these systems have received more attention in the past two decades. In order to have a better efficiency with lower costs and environmental impact, hybrid heat pumps are developed: a compressor is integrated in the cycle, increasing the efficiency of the system so part of produced vapor in evaporator follows an alternative compression cycle.

In this research, a mathematical model and a simulation of absorption and hybrid heat pumps are carried out with ChemCad® 6.0.1. The working fluid LiBr-H₂O, being non-toxic, at 56wt% is used, avoiding crystallization phenomena during the operations of systems. In the simulations, electrolyte's latent heat is used as enthalpy model, and electrolyte's non-random two-liquid model is used to calculate activity

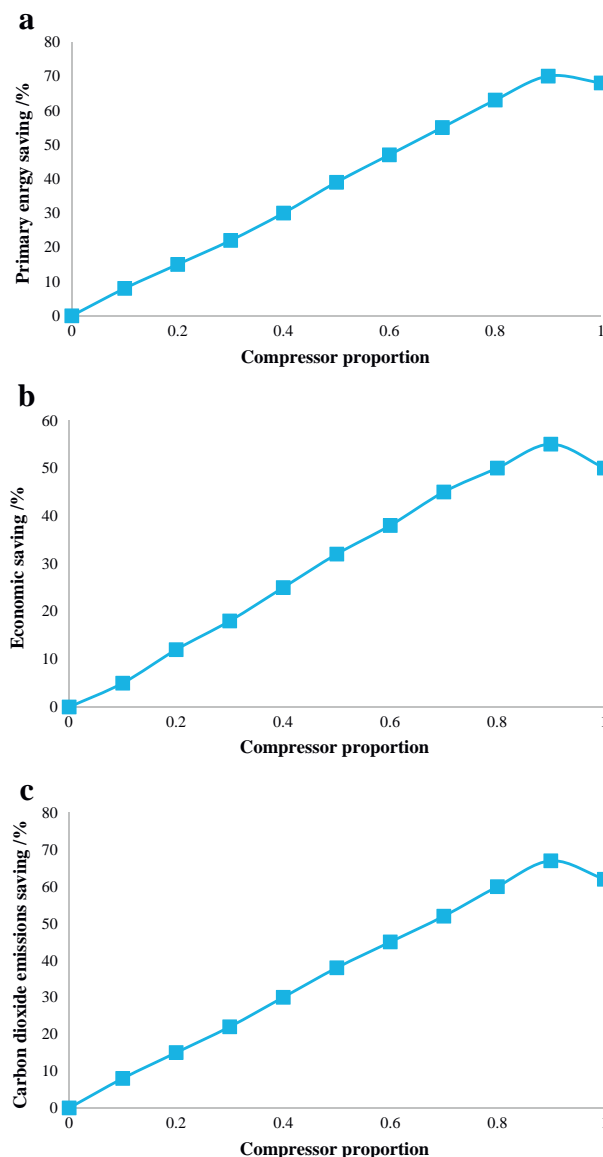


Fig. 15. Primary energy saving a), economic saving b), carbon dioxide emissions saving c) of hybrid heat pump respect to absorption heat pump versus CP.

coefficients involved in the vapor–liquid equilibrium. In fact, this model is more accurate with respect to Pitzer thermodynamic model for electrolytic solutions. The binary parameters of the activity coefficients are regressed from vapor pressure data while default equilibrium constant coefficients are used for the calculation of solubility of salt. Material and energy balances are obtained by the simulations of the systems. Results show that from a sensitivity analysis, it is found that the COP of absorption heat pump increases with the increase of generator temperature until reaching an asymptotic value and it is higher for lower generator pressure; the cooling capacity increases with the generator temperature and with the decrease of LiBr content in water. The absorption heat pump has a cooling capacity equal to 216 kW with a generator and absorber temperature equal to 358 K and 306 K respectively.

Hybrid heat pump has two different COPs: thermal and mechanic and from a sensitivity analysis is found that the thermal COP is strongly influenced by compressor proportion and increases with this parameter while the mechanic COP decreases with CP. Other important parameters for hybrid heat pump are primary energy ratio and heat and electrical energy supplied to the generator and

compressor respectively. The PER is linear with the CP and decrease until to minimum value where the hybrid heat pump works with the maxim efficiency. The heat supplied to generator has a linear decreasing with compressor proportion, while compressor power has a linear increasing with CP. The cooling capacity of the hybrid heat pump is 261 kW, the generator and absorber temperature is respectively equal to 358 K and 306 K too.

Also, results show that the hybrid heat pump provides energetic, environmental and economic advantages with respect to a conventional absorption heat pump: in correspondence to the compressor proportion limit value, it allows to save the 57%, 70%, and 67% of costs, primary energy and carbon dioxide emissions respectively.

Future researches should focus on the construction of this heat pumps integrated in chemical processes as a biogas plant or trigeneration systems. The biogas thermal power can be sent to the generator in order to produce heat, electricity and cold. Optimization studies should be carried out to realize an efficient system.

Acknowledgments

The author of the study would like to thank the European Commission for funding this work.

References

- [1] R. Tozer, R.W. James, Fundamental thermodynamics of ideal absorption cycles, *Int. J. Refrig.* 20 (1997) 120–135.
- [2] V. Tufano, Simplified criteria for the development of new absorption working pairs, *Appl. Therm. Eng.* 18 (1998) 171–177.
- [3] A. Costa, B. Bakhtiari, S. Schuster, J. Paris, Integration of absorption heat pumps in a Kraft pulp process for enhanced energy efficiency, *Energy* 34 (2009) 254–260.
- [4] P. Srihirin, S. Aphornratana, S. Chungpaibulpatana, A review of absorption refrigeration technologies, *Renew. Sust. Energy. Rev.* 5 (2001) 343–372.
- [5] J.T. Mc Mullan, Refrigeration and the environment-issues and strategies for the future, *Int. J. Refrig.* 25 (2002) 89–99.
- [6] G.A. Floride, S.A. Kalogirou, S.A. Tassou, L.C. Wrobel, Modelling, simulation 460 and warming impact assessment of a domestic-size absorption solar cooling system, *Appl. Therm. Eng.* 22 (2002) 1313–1325.
- [7] N.A. Darwish, S.H. Al-Hashimi, A.S. Al-Mansoori, Performance analysis and evaluation of a commercial absorption-refrigeration water-ammonia (ARWA) system, *Int. J. Refrig.* 7 (2008) 1214–1223.
- [8] D.S. Kim, C.A. Infante Ferreira, Analytic modelling of steady state single-effect absorption cycles, *Int. J. Refrig.* 31 (6) (2008) 1012–1020.
- [9] X. Zhang, D. Hu, Performance analysis of the single-stage absorption heat transformer using a new working pair composed of ionic liquid and water, *Appl. Therm. Eng.* 37 (2012) 129–135.
- [10] J. Sun, L. Fu, S. Zhang, W. Hou, A mathematical model with experiments of single effect absorption heta pump using LiBr-H₂O, *Appl. Therm. Eng.* 30 (2010) 2753–2762.
- [11] J.L. Rodríguez-Muñoz, J.M. Belman-Flores, Review of diffusion-absorption refrigeration technologies, *Renew. Sust. Energy. Rev.* 30 (2014) 145–153.
- [12] H.M. Hellmann, F. Ziegler, Simple absorption heat pump modules for system simulation programs, *ASHRAE Trans.* (1999) 780–787.
- [13] O. Kaynakli, M. Kilic, Theoretical study on the effect of operating conditions on performance of absorption refrigeration system, *Energy Convers. Manag.* 48 (2) (2007) 599–607.
- [14] Z. Kravanja, I.E. Grossmann, Computational approach for the modelling/decomposition strategy in the MINLP optimization of process flowsheets with implicit models, *Ind. Eng. Chem. Res.* 35 (1996) 2065–2070.
- [15] M.S. Diaz, J.A. Bandon, A mixed integer optimization strategy for a large chemical plant in operation, *Comput. Chem. Eng.* 20 (1996) 531–545.
- [16] J.A. Caballero, D. Milan-Yanez, I.E. Grossmann, Rigorous design of distillation columns: Integration of disjunctive programming and process simulators, *Ind. Eng. Chem. Res.* 44 (2005) 6760–6775.
- [17] H. Kim, I.H. Kim, E.S. Yoon, Multi objective design of calorific value adjustment process using process simulators, *Ind. Eng. Chem. Res.* 49 (2010) 2841–2848.
- [18] R. Brunet, G. Guillen-Gosalbez, L. Jimenez, Cleaner design of single-product biotechnological facilities through the integration of process simulation, multi objective optimization, life cycle assessment, and principal component analysis, *Ind. Eng. Chem. Res.* 51 (2012) 410–424.
- [19] S.C. Kaushik, A. Arora, Energy and exergy analysis of single effect and series flow double effect water-lithium bromide absorption refrigeration systems, *Int. J. Refrig.* 32 (2009) 1247–1258.
- [20] A. Arora, S.C. Kaushik, Theoretical analysis of LiBr/H₂O absorption refrigeration systems, *Int. J. Energy Res.* 33 (15) (2009) 1321–1340.
- [21] B. Borgas, Development of the Hybrid Absorption Heat Pump Process at High Temperature Operation, Norwegian University of Science and Technology, Department of Energy and Process Engineering, 2014.
- [22] D. Boer, M. Valles, A. Coronas, Performance of double effect absorption compression cycles for air-conditioning using methanol-TEGDME and TFE-TEGDME systems as working pairs, *Int. J. Refrig.* 21 (7) (1998) 542–555.
- [23] R. Ayala, C.L. Heard, F.A. Holland, Ammonia/lithium nitrate absorption/compression refrigeration cycle. Part I. Simulation, *Appl. Therm. Eng.* 17 (1997) 223–233.
- [24] G. Maurer, Electrolyte solutions, *Fluid Phase Equilib.* 13 (1983) 269–296.
- [25] E.A. Guggenheim, The specific thermodynamic properties of aqueous solutions of strong electrolytes, *Philos. Mag.* 19 (1935) 588–643.
- [26] J.N. Bronstedt, J. Amer, Calculation of the osmotic and activity functions in solutions of uni-univalents salts, *J. Am. Chem. Soc.* 44 (5) (1922) 938–948.
- [27] L.A. Bromley, Approximate individual ion values of β (or B) in extended Debye-Hückel theory for uni-univalent aqueous solutions at 298.15 K, *J. Chem. Thermodyn.* 4 (5) (1972) 669–673.
- [28] K.S. Pitzer, Thermodynamics of electrolyte. I. Theoretical basis and general equations, *J. Phys. Chem.* 77 (1973) 268–277.
- [29] J.L. Cruz, H. Renon, New thermodynamic representation of binary electrolyte – Solutions non-ideality in whole range of concentrations, *AIChE J.* 24 (1978) 817–830.
- [30] F.X. Ball, W. Furst, H. Renon, An NRTL model for representation and prediction of deviation from ideality in electrolyte solutions compared to the models of Chen (1982) and Pitzer (1973), *AIChE J.* 31 (1985) 392–399.
- [31] C.C. Chen, L.B. Evans, A local composition model for the excess Gibbs energy of aqueous-electrolyte systems, *AIChE J.* 32 (1986) 444–454.
- [32] A. Haghtalab, J.H. Vera, A nonrandom factor model for the excess Gibbs energy of electrolyte solutions, *AIChE J.* 34 (1988) 803–813.
- [33] Y. Liu, A.H. Harvey, J.M. Prausnitz, Thermodynamics of concentrated electrolyte solutions, *Chem. Eng. Commun.* 77 (1989) 43–66.
- [34] B. Sander, P. Rasmussen, A. Fredenslund, Calculation of vapor-liquid Equilibria in nitric-acid water nitrate salt systems using an extended Uniquac equation, *Chem. Eng. Sci.* 41 (1986) 1185–1195.
- [35] E.A. Macedo, P. Skovborg, P. Rasmussen, Calculation of phase equilibria for solutions of strong electrolytes in solvent-Water mixtures, *Chem. Eng. Sci.* 45 (1990) 875–882.
- [36] J.F. Zemaitis Jr., D.M. Clark, M. Rafal, N.C. Scrivner, Handbook of Aqueous Electrolyte Thermodynamics, DIPPR, AIChE, New York, 1986.
- [37] H. Renon, Electrolyte solutions, *Fluid Phase Equilib.* 30 (1986) 181–195.
- [38] K.S. Pitzer, Activity Coefficients in Electrolyte Solutions, 2nd edition CRC Press, Boca Raton, FL, 1991.
- [39] M. Rafal, J.W. Berthold, N.C. Scrivner, S.L. Grise, Models for Electrolyte Solutions, in: S.I. Sandler (Ed.), Models for Thermodynamic and Phase Equilibria Calculations, Marcell Dekker, New York 1994, p. 601.
- [40] J.R. Loeh, M.D. Donohue, Recent advances in modeling thermodynamic properties of aqueous strong electrolyte systems, *AIChE J.* 43 (1997) 180–195.
- [41] B.E. Conway, J.O'M. Bockris, E. Yeag, S.U.M. Kham, R.E. White, Comprehensive Treatise of Electrochemistry, Plenum Press, New York, 1983.
- [42] R.M. Mazo, C.Y. Mou, in: K.S. Pitzer (Ed.), Activity coefficients in electrolyte solutions, 2nd edition CRC Press, Boca Raton, FL, 1991.
- [43] G. Grossman, K.W. Childs, Computer simulation of a lithium bromide-water absorption heat pump for temperature boosting, *ASHRAE Trans.* 89 (1b) (1983) 240–248.
- [44] G. Grossman, Modular Simulation of Absorption Systems. User's Guide and Reference Windows. Version 5.0 (AbsimW), 1998.
- [45] M.O. Mc Linden, S.A. Klein, Steady state modeling of absorption heat pumps with a comparison to experiments, *ASHRAE Trans.* 91 (2b) (1985) 1793–1807.
- [46] H. Perez-Blanco, M.R. Patterson, Conceptual Design and Optimization of a Versatile Absorption Heat Transformer. ORNL/TM-9841, Oak Ridge National Laboratory, 1986.
- [47] G.C. Vliet, M.B. Lawson, R.A. Lithgow, Water-lithium bromide double effect absorption cooling cycle analysis, *ASHRAE Trans.* 88 (1) (1982) 811–823.
- [48] J.D. Marcos, M. Izquierdo, E. Palacios, New method for COP optimization in water-and air-cooled single and double effect LiBr-water absorption machines, *Int. J. Refrig.* 34 (2011) 1348–1359.
- [49] R. Gomri, Second law comparison of single effect and double effect vapour absorption refrigeration systems, *Energy Convers. Manag.* 50 (2009) 1279–1287.
- [50] L.M. Chavez-Islas, C.L. Heard, Optimization of a simple ammonia-water absorption refrigeration cycle by application of mixed-integer nonlinear programming, *Ind. Eng. Chem. Res.* 48 (4) (2009) 1957–1972.
- [51] L.M. Chavez-Islas, C.L. Heard, I.E. Grossmann, Synthesis and optimization of an ammonia/water absorption refrigeration cycle considering different types of heat exchangers by application of mixed-integer nonlinear programming, *Ind. Eng. Chem. Res.* 48 (6) (2009) 2972–2990.
- [52] B.H. Gebreslassie, G. Guillen-Gosalbez, L. Jimenez, D. Boer, Design of environmentally conscious absorption cooling systems via multi-objective optimization and life cycle assessment, *Appl. Energy* 86 (9) (2009) 1712–1722.
- [53] B.H. Gebreslassie, G. Guillen-Gosalbez, L. Jimenez, D. Boer, Economic performance optimization of an absorption cooling system under uncertainty, *Appl. Therm. Eng.* 29 (17–18) (2009) 3491–3500.
- [54] A. Brooke, D. Kendrick, A. Meeraus, GAMS e a User's Guide (Release 2.25), The Scientific Press, San Francisco, 1996.
- [55] P.I. Barton, C.C. Pantelides, gPROMS e a combined discrete/continuous modeling environment for chemical processing systems, *Simul. Ser.* 25 (3) (1993) 25–34.
- [56] R. Fourer, D.M. Gay, B.W. Kernighan, A modeling language for mathematical programming, *Manag. Sci.* 36 (1990) 519–554.
- [57] C.R. Maya, J.J. Pacheco-Ibarra, J.M. Belman-Flores, S.R. Galván-González, C. Mendoza-Covarrubias, NLP model of a LiBr-H₂O absorption refrigeration system for the minimization of the annual operating cost, *Appl. Therm. Eng.* 37 (2012) 10–18.
- [58] M.S. Mazzei, M.C. Mussati, S.F. Mussati, NLP model-based optimal design of LiBr-H₂O absorption refrigeration systems, *Int. J. Refrig.* 38 (2014) 58–70.

- [59] A. Kodal, B. Sahin, A.S. Oktem, Performance analysis of two stage combined heat pump system based on thermo-economic optimization criterion, *Energy Convers. Manag.* 41 (18) (2000) 1989–2008.
- [60] A. Kodal, B. Sahin, A. Erdil, Performance analysis of a two stage irreversible heat pump under maximum heating load per unit total cost conditions, *Int. J. Exergy* 2 (3) (2002) 159–166.
- [61] A. Kodal, B. Sahin, I. Ekmekeci, T. Yilmaz, Thermo economic optimization for irreversible absorption refrigerator and heat pumps, *Energy Convers. Manag.* 44 (1) (2003) 109–123.
- [62] R.D. Misra, P.K. Sahoo, S. Sahoo, A. Gupta, Thermo economic optimization of a single effect water/LiBr vapour absorption refrigeration system, *Int. J. Refrig.* 26 (2) (2003) 158–169.
- [63] R.D. Misra, P.K. Sahoo, S. Sahoo, A. Gupta, Thermo economic evaluation and optimization of a double-effect H₂O/LiBr vapour-absorption refrigeration system, *Int. J. Refrig.* 28 (3) (2005) 331–343.
- [64] R.D. Misra, P.K. Sahoo, S. Sahoo, A. Gupta, Thermo economic evaluation and optimization of an aqua-ammonia vapour absorption refrigeration system, *Int. J. Refrig.* 29 (1) (2006) 47–59.
- [65] B. Sahin, A. Kodal, Thermo economic optimization of a two stage combined refrigeration system: A finite-time approach, *Int. J. Refrig.* 25 (7) (2002) 872–877.
- [66] O. Kizilkan, A. Sencan, S.A. Kalogirou, Thermo economic optimization of a LiBr absorption refrigeration system, *Chem. Eng. Process.* 46 (12) (2007) 1376–1384.
- [67] R. Palacios Bereche, R. Gonzales Palomino, S.A. Nebra, Thermo economic analysis of a single and double-effect LiBr/H₂O absorption refrigeration system, *Int. J. Thermodyn.* 12 (2) (2009) 89–98.
- [68] C.M.R. Varani, C.A.C. Santos, R.R. Gondim, E.A. Torres, Energetic and exergetic evaluation of a lithium bromide/water absorption refrigeration system utilizing natural gas, *Proc. of ECOS2003*, Copenhagen, Denmark, June 30–July 2 2003, pp. 1597–1619.
- [69] P.K. Sahoo, R.D. Misra, A. Gupta, Exergoeconomic optimisation of an aqua-ammonia absorption refrigeration system, *Int. J. Exergy* 1 (1) (2005) 82–93.
- [70] D.A. Al-Otaibi, I. Dincer, M. Kalyon, Thermo-economic optimization of vapor-compression refrigeration systems, *Int. Commun. Heat Mass Transfer* 31 (1) (2004) 95–107.
- [71] S. Jeong, B.H. Kang, S.W. Karng, Dynamic simulation of an absorption heat pump for recovering low-grade waste heat, *Appl. Therm. Eng.* 18 (1998) 1–12.
- [72] D.G. Fu, G. Poncia, Z. Lu, Implementation of an object-oriented dynamic modeling library for absorption refrigeration systems, *Appl. Therm. Eng.* 26 (2006) 217–225.
- [73] P. Kohlenbach, F. Ziegler, A dynamic simulation model for transient absorption chiller performance. Part I: The model, *Int. J. Refrig.* 31 (2008) 217–225.
- [74] P. Kohlenbach, F. Ziegler, A dynamic simulation model for transient absorption chiller performance. Part II: Numerical results and experimental verification, *Int. J. Refrig.* 31 (2008) 226–233.
- [75] Y. Takagi, T. Nakamaru, Y. Nishitani, An absorption chiller model for HVACSIM+, IBPSA Conference 1999, Kyoto, Japan, September 13–15, 1999.
- [76] A. Palau, E. Velo, L. Puigjaner, Use of neural networks and expert systems to control a gas/solid sorption chilling machine, *Int. J. Refrig.* 22 (1999) 59–66.
- [77] A. Myat, K. Thu, Y.D. Kim, A. Chakraborty, W.G. Chun, K.C. Ng, A second law analysis and entropy generation minimization of an absorption chiller, *Appl. Therm. Eng.* 31 (2011) 2405–2413.
- [78] G. Evola, N. Le Pierré, F. Boudehenn, P. Papillon, Proposal and validation of a model for the dynamic simulation of a solar-assisted single-stage LiBr/water absorption chiller, *Int. J. Refrig.* 36 (2013) 1015–1028.
- [79] M. Zinet, R. Rulliere, P. Haberschill, A numerical model for the dynamic simulation of a recirculation single effect absorption chiller, *Energy Convers. Manag.* 62 (2012) 51–63.
- [80] J. Seo, Y. Shin, J. Dong Chung, Dynamics and control of solution levels in a high temperature generator for an absorption chiller, *Int. J. Refrig.* 35 (2012) 1123–1129.
- [81] A. Iranmanesh, M.A. Mehrabian, Thermodynamic modelling of a double-effect LiBr–H₂O absorption refrigeration cycle, *Heat Mass Transf.* 48 (12) (2012) 2113–2123.
- [82] A. Iranmanesh, M.A. Mehrabian, Dynamic simulation of a single-effect LiBr–H₂O absorption refrigeration cycle considering the effects of thermal masses, *Energy Build.* 60 (2013) 47–59.
- [83] V. Congradac, F. Kulic, Recognition of the importance of using artificial neural networks and genetic algorithms to optimize chiller operation, *Energy Build.* 47 (2012) 651–658.
- [84] O. Kaynakli, R. Yamankaradeniz, Thermodynamic analysis of absorption refrigeration system based on entropy generation, *Curr. Sci.* 92 (4) (2007) 472–479.
- [85] S. Aphornratana, T. Sriveerakul, Experimental studies of a single-effect absorption refrigerator using aqueous lithium–bromide: Effect of operating condition to system performance, *Exp. Thermal Fluid Sci.* 32 (2007) 658–669.
- [86] M.I. Karamangil, S. Coskun, O. Kaynakli, N. Yamankaradeniz, A simulation study of performance evaluation of single-stage absorption refrigeration system using conventional working fluids and alternatives, *Renew. Sust. Energ. Rev.* 14 (2010) 1969–1978.
- [87] K. Klein, K. Huchtemann, D. Muller, Numerical study on hybrid heat pump systems in existing buildings, *Energy Build.* 69 (2014) 193–201.
- [88] G. Bagarella, R. Lazzarin, M. Noro, Annual simulation, energy and economic analysis of hybrid heat pump systems for residential buildings, *Appl. Therm. Eng.* 99 (2016) 485–494.
- [89] F. Ziegler, G. Hammer, Experimental results of a double-lift absorption heat pump, *Proc. 4th International Conf. On Application and Efficiency of Heat Pump Systems in Environmentally Sensitive Times*, Munich, Germany 1991, pp. 49–58 (1–3 October).
- [90] R. Ayala, An Experimental Study of Heat Driven Absorption Cooling Systems. PhD Thesis University of Salford, UK, 1995.
- [91] A. Jaretun, G. Aly, New local composition model for electrolyte solutions: Multicomponent systems, *Fluid Phase Equilib.* 175 (2000) 213–228.
- [92] C.C. Chen, Y.S. Somerville, Computer method and system for predicting physical properties using a conceptual segment-based ionic activity coefficient model, *US 7,809,540 B2*, Oct. 5, 2010.
- [93] A. Jaretun, G. Aly, New local composition model for electrolyte solutions: Single solvent, single electrolyte systems, *Fluid Phase Equilib.* 163 (1999) 175–193.
- [94] C.C. Chen, Computer method and system for predicting physical properties using a conceptual segment model, *US 8,666,675 B2*, Mar. 4, 2014.
- [95] C.C. Chen, Y.S. Somerville, Method of modelling physical properties of chemical mixtures and articles of use, *US 8,346,525 B2*, Jan. 1, 2013.
- [96] J.M. Prausnitz, R.N. Lichtenthaler, E.G. de Azevedo, *Molecular Thermodynamics of Fluid Phase Equilibria*, third ed. Prentice Hall, New Jersey, 1999 537–556.
- [97] D.W. Sun, Thermodynamic design data and optimum design maps for absorption refrigeration systems, *Appl. Therm. Eng.* 17 (1997) 211–221.
- [98] G. Leonzio, Recovery of base metal sulphates and hydrochloric acid regeneration from spent pickling liquors: Process simulation, *J. Clean. Prod.* 129 (2015) 417–426.
- [99] K.E. N'Tsoukpoe, M. Perier-Muzet, N. Le Pierres, L. Luo, D. Mangin, Thermodynamic study of a LiBr–H₂O absorption process for solar heat storage with crystallisation of the solution, *Sol. Energy* 104 (2014) 2–15.
- [100] A.M.K. Bahman, Modeling of Solar-Powered Single-Effect Absorption Cooling System and Supermarket Refrigeration/HVAC System, PhD Thesis, University of South Florida, 2011.
- [101] T. Berlitz, B. Cerkvénik, H.M. Hellmann, F. Ziegler, The impact of work input sorption cycles, *Int. J. Refrig.* 24 (2001) 88–99.
- [102] K.E. Herold, R. Radermacher, S.A. Klein, *Absorption Chillers and Heat Pumps*, CRC Press Inc., 1996.
- [103] B. Bakhtiari, L. Fradette, R. Legros, J. Paris, A model for analysis and design of H₂O–LiBr absorption heat pumps, *Energy Convers. Manag.* 52 (2011) 1439–1448.
- [104] W. Wu, X. Zhang, X. Li, W. Shi, B. Wang, Comparisons of different working pairs and cycles on the performance of absorption heat pump for heating and domestic hot water in cold regions, *Appl. Therm. Eng.* 48 (2012) 349–358.
- [105] Z. Hariz, Analysis of Absorption Chiller for Heat Recovery Purpose, Final Year Project, Faculty of Engineering-Branch III – Lebanese University, Lebanon, 2003.
- [106] N. Zang, K. Wang, N. Lior, W. Han, Performance study and energy saving mechanism analysis of an absorption/mechanical hybrid heat pump cycle, The 28th International Conference on Efficiency, Cost, Optimization, Simulation and Environmental Impact of Energy Systems, June 30–July 3, Pau, France, 2015.
- [107] D. Boer, M.H. Huor, M. Prevost, A. Coronas, Combined vapour-compression-double effect absorption cycle for air conditioning: a new high performance cycle, *Proc. IAHP Conf.*, New Orleans, LA. ASME, AES 31 1994, pp. 483–486.
- [108] N. Sawada, K. Minato, Y. Kunugi, T. Mochizuki, T. Kashiwagi, Cycle simulation/COP evaluation of compression hybrid Heat pump: heat amplifier type, in: *Proceedings of the International Absorption Heat Pump Conference (Ed.)* 31, ASME AES, New Orleans 1994, pp. 471–476.